2017-09

Distinct phenotypes of three-repeat and four-repeat human tau in a transgenic model of tauopathy

Sealey, MA

10.1016/j.nbd.2017.05.003
Neurobiology of Disease
Elsevier BV

Neurobiology of Disease 105 (2017) 74–83

Contents lists available at ScienceDirect

Neurobiology of Disease

journal homepage: www.elsevier.com/locate/ynbdi

Distinct phenotypes of three-repeat and four-repeat human tau in a transgenic model of tauopathy

Megan A. Sealey [a], Ergina Vourkou [c], Catherine M. Cowan [a], Torsten Bossing [b], Shmma Quraishe [a], Sofia Grammenoudi [c], Efthimios M.C. Skoulakis [c], Amritpal Mudher [a,*]

[a] Centre for Biological Sciences, University of Southampton, Southampton SO17 1BJ, UK
[b] School of Biomedical and Healthcare Sciences, Plymouth University, PL6 8BU, UK
[c] Division of Neuroscience, Biomedical Sciences Research Centre "Alexander Fleming", Vari 16672, Greece

ARTICLE INFO

Article history:
Received 1 December 2016
Revised 12 April 2017
Accepted 10 May 2017
Available online 11 May 2017

Keywords:
3R tau
4R tau
Alzheimer's disease
Drosophila
Isoforms
Tauopathy

ABSTRACT

Tau exists as six closely related protein isoforms in the adult human brain. These are generated from alternative splicing of a single mRNA transcript and they differ in the absence or presence of two N-terminal and three or four microtubule binding domains. Typically all six isoforms have been considered functionally similar. However, their differential involvement in particular tauopathies raises the possibility that there may be isoform-specific differences in physiological function and pathological role. To explore this, we have compared the phenotypes induced by the 0N3R and 0N4R isoforms in *Drosophila*. Expression of the 3R isoform causes more profound axonal transport defects and locomotor impairments, culminating in a shorter lifespan than the 4R isoform. In contrast, the 4R isoform leads to greater neurodegeneration and impairments in learning and memory. Furthermore, the phosphorylation patterns of the two isoforms are distinct, as is their ability to induce oxidative stress. These differences are not consequent to different expression levels and are suggestive of bona fide physiological differences in isoform biology and pathological potential. They may therefore explain isoform-specific mechanisms of tau-toxicity and the differential susceptibility of brain regions to different tauopathies.

1. Introduction

Transcripts from the single microtubule associated protein tau (MAPT)-encoding gene on human chromosome 17q21.1 are spliced into six isoforms in the adult brain (Andreadis, 2005). These tau isoforms, ranging in size from 352 to 441 amino acids, arise because of alternative splicing of exons 2, 3 and 10 leading to the absence or presence of 1 or 2 N-terminal domains and 3 or 4C-terminal microtubule binding repeats (Goedert et al., 1989). They are commonly referred to as 0N3R, 1N3R, 2N3R, 0N4R, 1N4R and 2N4R tau. Furthermore, tau isoforms undergo a variety of post-translational modifications including Ser/Thr and Tyr phosphorylation, acetylation and SUMOylation. Some of these modifications occur physiologically and are regulated during development and aging; others occur in pathological conditions and are implicated in tau-mediated toxicity (reviewed in (Medina et al., 2016; Huefner et al., 2013)).

It has been argued that regulation of alternative splicing during development is a mechanism for radically altering the function of tau protein. This may be reflected in expression of 3R isoforms early in human brain development during axon path finding when a more dynamic cytoskeleton is required and then transitioning to expression of 4R isoforms post neurite elaboration, when a more stable network has been established (Andreadis, 2005). Accordingly, a main distinction of tau isoforms involves differentiation of the microtubule-binding repeats. This likely underlies differences in isoform physiology and pathological potential as they ostensibly interact with distinct or partially overlapping membrane-associated, cytosolic and cytoskeletal proteins. In fact, differences in microtubule binding properties were well-known (Goode et al., 2000), but several studies have now demonstrated additional isoform-specific differences including: the propensity of tau to aggregate (Adams et al., 2010), differential templated seeding capabilities (Dinkel et al., 2011), intra-neuronal re-localisation during tangle formation (Hara et al., 2013; Liu and Gotz, 2013), interactions with distinct cellular binding partners (Bhaskar et al., 2005; Liu et al., 2016), phosphorylation potential and the impact of these differences on their biochemical properties (Combs et al., 2011).

The ratio of 3R to 4R isoforms in the adult human brain is approximately 1. The equimolar isoform ratio is disrupted in some familial tauopathies due to splicing mutations, which lead to elevation of the 4R tau isoforms (Andreadis, 2005). Even in Alzheimer's Disease (AD) there is evidence of impaired 3R/4R ratio in tangle bearing neurons (Niblock and Gallo, 2012; Park et al., 2016). The fact that disrupting

* Corresponding author.
E-mail address: A.Mudher@soton.ac.uk (A. Mudher).
Available online on ScienceDirect (www.sciencedirect.com).

http://dx.doi.org/10.1016/j.nbd.2017.05.003

the isoform ratio is associated with disease, demonstrates the importance of maintaining the 3R:4R isoform balance in healthy neurons. Additionally, not all isoforms are present in tau aggregates that characterise particular tauopathies, including sporadic forms. In AD for example, all tau isoforms form filaments, whereas in others they are comprised predominately of either 3R (e.g. Pick's disease), or 4R isoforms (e.g. Progressive Supranuclear Palsy, Corticobasal Degeneration, Argyrophilic Grain Disease) (Rabano et al., 2013; Spillantini and Goedert, 2013).

When divergent phenotypes are reported in animal models of tauopathy, the particular isoform expressed is not typically considered as a reason for the discrepancy. Here we highlight this by systematically assessing isoform-specific phenotypes in *Drosophila* and demonstrate that distinct tau isoforms can have significantly different effects in identical assays. This may shed light on the role of isoform-specific differences in the divergent pathogenic profiles of tauopathies where one of these isoforms predominates.

2. Materials and methods

2.1. Flies

Female *Drosophila melanogaster* expressing either the motor neuron-specific driver D42-GAL4, pan-neuronal driver Elav^{C155}-GAL4 and Elav^{C155}-GAL4/TubGAL80^{ts} (Bloomington Stock Centre), sensory neuron driver panR7-GAL4 or retinal photoreceptor driver GMR-GAL4 were crossed with male flies transgenic for UAS-human 0N3R tau (UAS-hTau^{0N3R}), or UAS-human 0N4R tau (two 4R transgenic lines were used and they are referred to as hTau^{0N4R} and hTau^{0N4R*}; they are distinct transgene insertions presenting similar expression levels – see Suppl. Fig. 1), or with wild-type Oregon-R male flies (WT). All transgenic lines and drivers were obtained from the Bloomington Stock centre (USA), except the UAS-htau^{0N4R} and UAS-htau^{0N4R*} lines, which were originally generated by Prof. Mel Feany (Brigham and Women's Hospital, Boston, USA).

2.2. Larval locomotion analysis

As previously described (Sinadinos et al., 2012), wandering third instar larvae were allowed to crawl freely in a 10 cm × 10 cm plate, filled to a depth of approximately 4 mm with dark blue agarose (1% agarose, 0.1% alcian blue), within a bioassay room kept at 21 °C, 30–40% humidity, and controlled lighting conditions. After a 6-minute acclimatisation period, larvae were placed at the centre of the plate, and were filmed for 2 min using an Ikegami digital video camera and 5 mm camera lens (Tracksys, UK). 4 such plates were filmed simultaneously. Ethovision movement analysis software (Noldus Information Technology) was then used to measure the following parameters of locomotion: velocity (mm/s); meander, measured as the angle deviated from the straight path per cm travelled (degrees/cm); and angular velocity (degrees/s). Further, the frequency of contractions of the body-wall muscles (contractions/min) was measured semi-manually from these video recordings, with the experimenter blinded to condition. GraphPad Prism was used to calculate standard error of the mean, unpaired 2-tailed students *t*-test, and/or 1-way ANOVA on the resulting data, as appropriate.

2.3. Adult climbing assay

This assay was performed on cohorts of 15 adult flies, which had been allowed to mate for 1–2 days after eclosion and then separated

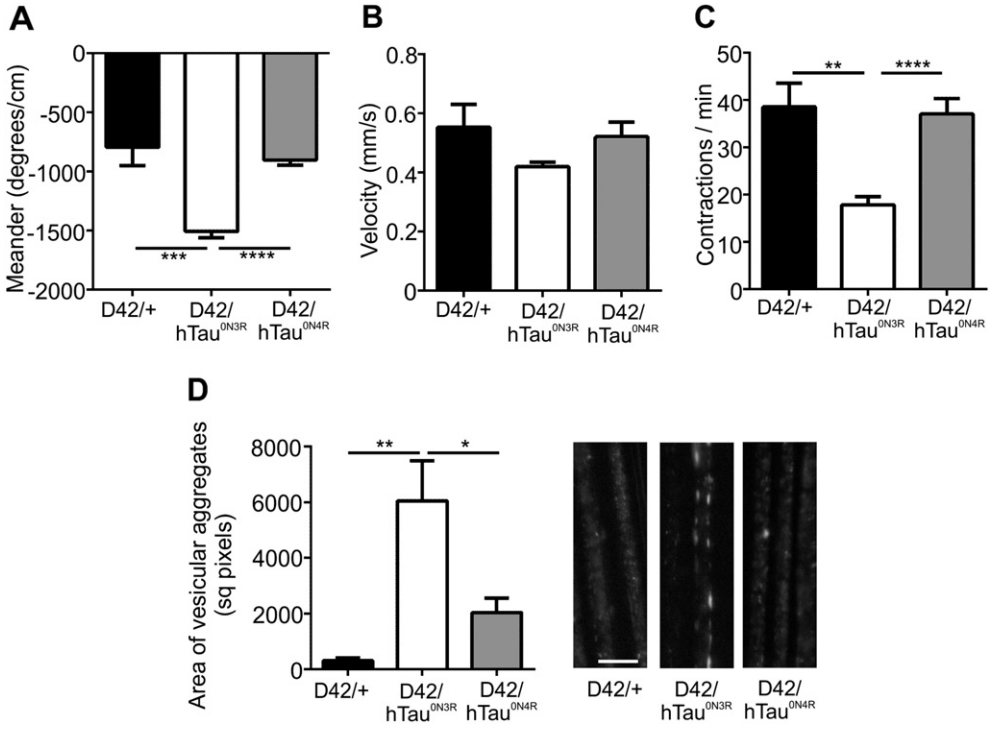

Fig. 1. *Drosophila* expressing hTau^{0N3R} but not hTau^{0N4R} in motor neurons display a motor phenotype, and impaired fast axonal transport. Locomotor performance in a free-crawling test is significantly impaired in hTau^{0N3R} -expressing larvae compared to controls in terms of meander (A), and frequency of body-wall contractions (C). In contrast locomotion of hTau^{0N4R}-expressing larvae is not different from driver controls. A similar trend is seen for velocity of movement (B) but the differences between genotypes are not significant. (D) In larval motor neurons, vesicular aggregates (indicative of axonal transport defect) were found in hTau^{0N3R}-expressing larvae but not in controls or hTau^{0N4R}-expressing larvae. Very few aggregates were found in hTau^{0N4R}-expressing larvae compared to hTau^{0N3R}-expressing larvae. Scale bar = 10 μm. For meander: WT vs hTau^{0N3R} $p = 0.0009$; hTau^{0N3R} vs hTau^{0N4R} $p = 0.0001$; WT vs hTau^{0N4R} $p = 0.4801$. For velocity: WT vs hTau^{0N3R} $p = 0.1508$ (ns); hTau^{0N3R} vs hTau^{0N4R} $p = 0.0928$ (ns); WT vs hTau^{0N4R} $p = 0.7304$ (ns). For body wall contractions: WT vs hTau^{0N3R} $p = 0.0013$; hTau^{0N3R} vs hTau^{0N4R} $p = 0.0001$; WT vs hTau^{0N4R} $p = 0.803$ (ns) (Unpaired two-tailed *t*-tests; $n = 9$–10 per assay). For axonal transport: WT vs hTau^{0N3R} $p = 0.0041$; hTau^{0N3R} vs hTau^{0N4R} $p = 0.0306$; WT vs hTau^{0N4R} $p = 0.0116$ (Unpaired two-tailed *t*-tests or one-way Anova Bonferroni's multiple comparisons test $n = 5$). hTau^{0N3R} = {w / +; D42-GAL4 / +; UAShtau0N3R / +}. hTau^{0N4R} = {w / +; D42-GAL4 / +; UAShTau0N4R / + − parental line hTau^{0N4R}}. WT = {w / +; D42-GAL4 / +; + / +} on an OreR background.

by sex and housed in their testing cohorts. Each week, 6–9 h into the 12-hour light cycle of the flies, they were anaesthetised very briefly (<5 s) with CO_2 and placed in a measuring cylinder in an assay room with controlled lighting conditions, temperature (23 °C) and humidity (30–40%). They were given 15 min to recover from anaesthesia and to acclimatise to the assay room. The measuring cylinder was tapped 3 times upon a mouse pad to send the flies to the bottom, a video recording was carried out and paused 10s later when the analysis was conducted. Flies rested for 2 min, and the procedure was repeated 2 more times. Flies were then placed onto fresh food until the following week.

2.4. Survival assay

Three cohorts of 10 male flies of each genotype were separated 0–3 days post-eclosion and then transferred to new food twice a week and scored for deaths three times a week. Flies were housed in a room with controlled lighting conditions, temperature (23 °C) and humidity (30–40%). A Kaplan-Meier survival curve was plotted and a Log-rank (Mantel-Cox) test was performed on the data using GraphPad Prism software.

2.5. Adult learning and memory assay

To obtain animals for learning and memory assays UAS-hTau^{0N3R} and UAS-hTau^{0N4R} males were crossed *en masse* with Elav^{c155}GAL4; +;TubGAL80^{ts} at 18 °C. Upon eclosion they were collected in fresh bottles and tau expression was induced by placing the adult flies at 30 °C for 12 days with bottle changes every 3 days. On the 11th day the flies were separated in groups of 50–70 animals in vials and placed back at 30 °C overnight. All animals were placed in fresh food vials 1–2 h before conditioning. Conditioning assays were performed under dim red light at 24 °C–25 °C and 65%–75% humidity. All experiments were carried out in a balanced manner, where all genotypes involved in an experiment were tested per day. Classical learning refers to Pavlovian olfactory aversive conditioning and was performed using the aversive odors benzaldehyde (BNZ) and 3-octanol (OCT) diluted in oil (6% *v*/v for BNZ and 50% *v*/v for OCT) as conditioned stimuli (CS+ and CS−) with the electric shock unconditioned stimulus (US). For training, a group of 50–70 flies was first exposed to the CS+ odor for 40 s paired with 90 V shock (consisting of twelve 1.25 s pulses with 4.5 s inter-pulse intervals, therefore 8 US/CS pairings were delivered within 40 s of odor presentation) and then 30 s of air. Subsequently, flies were exposed to the CS− for 40 s without shock and then 30 s of air. Each experimental trial included two reciprocal groups, with the CS+ and CS− odors switched. Three minutes after conditioning, both groups of flies were tested simultaneously for preferential avoidance of the conditioned odorant.

For 24-hour memory experiments, flies were submitted to 12 US/CS pairings per round and five such rounds of training with a 15-minute inter-round interval. The flies were stored at 18 °C for 24 h and then transferred to a T-maze apparatus and allowed to choose between the two odors for 90 s. A performance index (PI) was calculated as the fraction of flies that avoided the CS+ minus the fraction that avoided the CS− odors divided by the total number of flies in the experiment. A final PI is the average of the scores from the two groups of flies trained with either benzaldehyde or 3-octanol as CS+ and ranges from 0 to 100.

2.6. Tau solubility assay to enrich for oligomeric tau species

This assay enriches for insoluble oligomeric tau species as described (Cowan et al., 2015). A total of 10 fly heads were homogenized in 40 μl of TBS/sucrose buffer (50 mM Tris-HCl pH 7.4, 175 mM NaCl, 1 M sucrose, 5 mM EDTA and protease inhibitor cocktail). The samples were then spun for 2 min at 1000 g and the pellet discarded. The supernatant was spun at 186,000 g for 2 h at 4 °C. The resulting supernatant was "S1" – the aqueous soluble fraction. The pellet was re-suspended at room temperature in 5% SDS/TBS buffer (50 mM Tris-HCl pH 7.4, 175 mM NaCl, 5% SDS) and spun at 186,000 g for 2 h at 25 °C. The resulting supernatant was "S2" – the SDS-soluble, aqueous-insoluble fraction. The pellet was resuspended at room temperature in 5% SDS/TBS buffer (50 mM Tris-HCl pH 7.4, 175 mM NaCl, 5% SDS and protease inhibitor cocktail) and spun at 186,000 g for 2 h at 25 °C as a wash spin; following which the supernatant was discarded. This pellet was then re-suspended in 8 M urea, 8% SDS buffer (50 mM Tris-HCl pH 7.4, 175 mM NaCl, 8% SDS, 8 M urea and protease inhibitor cocktail) and agitated for 12–18 h at room temperature ("S3"). All samples were diluted in 2× Laemmli buffer and boiled for 5 min. "S1" and "S2" were loaded equally (equivalent volumes) whereas double the amount of "S3" was loaded compared to "S1" and "S2". The S3 fraction was then quantified as a proportion of the sum total of all three fractions.

2.7. Protein oxidation assay (OxyBlot)

For each condition, 5 heads of 1 day-old flies were homogenized in 30 μl OxyBlot buffer (150 mM NaCl, 50 mM MES, 1% triton-X 100, 1% SDS, 2% β-mercaptoethanol, protease inhibitor cocktail). Homogenates were centrifuged for 5 min at 5000*g*, and the pellets discarded. 10 μl homogenate was used for a carbonyl derivatisation reaction with the OxyBlot kit (Millipore), according to the manufacturer's instructions. Briefly, we added 10 μl 12% SDS, 20 μl DNPH (or negative control

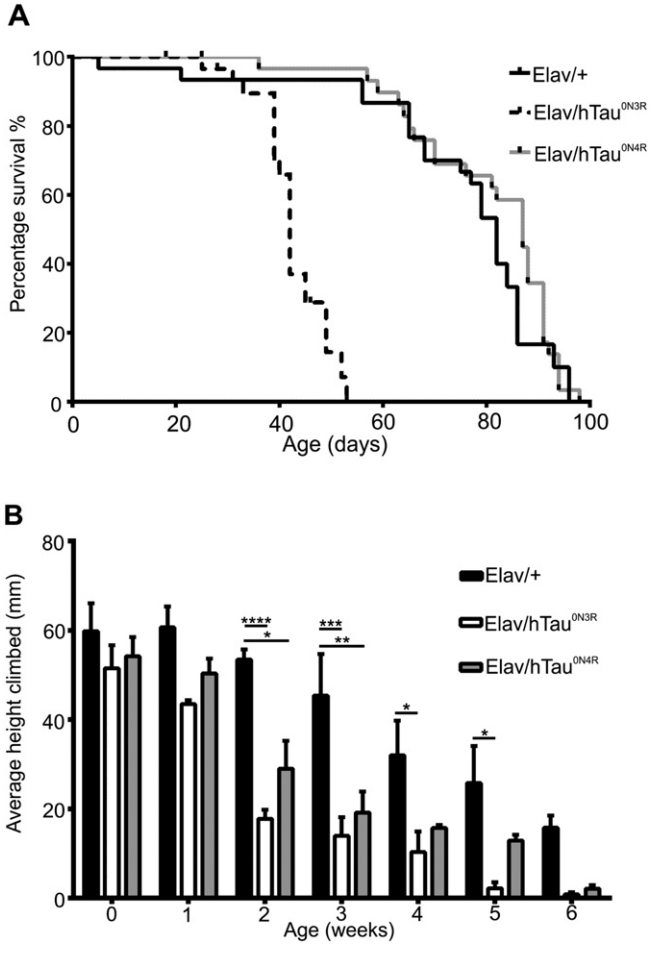

Fig. 2. Differential Tau isoform toxicity in adult *Drosophila*. (A) Survival curves for Elav-GAL4 driven hTau^{0N3R}, hTau^{0N4R} and WT male flies ($n = 30$). HTau^{0N3R} flies have significantly shorter lifespan compared with both htau^{0N4R} and WT flies (Log-rank, Mantel-Cox test $p = 0.0001$). B) Comparison of the climbing ability with age over 6 weeks for hTau^{0N3R}, hTau^{0N4R} and WT flies ($n = 30$). (2-way ANOVA; $p = 0.0002$). Error bars are plotted as ±S.E.M. hTau^{0N3R} = {w / +; Elav-GAL4 / +; UAShtau0N3R / +}. hTau^{0N4R} = {w / +; Elav-GAL4 / +; UAShTau^{0N4R} / + − parental line hTau^{0N4R}}. WT = {w / +; Elav-GAL4 / +; + / +} on an OreR background.

provided) and incubated 15 min at room temperature; then added 14 μl of neutralizing solution. 10 μl of this final labelled product was applied to nitrocellulose membrane (Amersham) using a slot blot apparatus (BioRad). Membranes were probed with anti-DNP antibody (Millipore, 1:150), and signal was detected using fluorescently conjugated anti-rabbit secondary antibody (LICOR) and a LiCor scanner with Odyssey software. Resulting band densities were measured using Image J software.

2.8. Western blotting

Western blotting was performed to assess total tau levels, phosphorylation and solubility state of tau. For Western blot analysis of larval samples, 10 3rd instar larvae or heads of 1-3d adult flies were pooled and homogenized in 200 μl 1× Laemmli buffer, boiled at 95 °C for 5 min and centrifuged for 5 min at 14000 RPM, at RT. Proteins were separated by SDS-PAGE according to standard methods, and transferred to PVDF membrane by semi-dry transfer Anti-Syntaxin (Developmental Hybridoma Bank) at 1:3000 was used as loading control. Primary antibodies were used as follows: anti-human tau (Dako, 1:15,000 or T46, 1:3000). The phosphorylation-specific anti-tau antibodies Ser396/Ser404 (PHF-1) (a gift from Peter Davies, USA, 1:500), Ser396 (Source Biosciences, 1:2000), Ser202/Thr205 (AT8) (Thermo Scientific, 1:1000), Thr212/Ser214 (AT100) (Pierce Endogen, 1:1000), dephosphorylated at Ser199/Ser202/Thr205 (Tau-1) (Millipore, 1:2000), pS262 (Invitrogen, 1:1000). MC1 (a gift from Peter Davies, USA), was used at 1:200. Secondary antibodies were at 1:5000 and the signal detected by chemiluminescence (ECL plus).

2.9. Axonal transport studies

Wandering third instar (L3) larvae (day 5) were anaesthetised by placing larvae in a chamber containing cotton wool soaked in diethylether vapour for 15 min. Larvae were immobilised on glass slides in 1% agarose ventral face up and mounted under coverslips. Peripheral nerves were analysed between the 2nd and 4th denticle bands. For total area acquisition, vGFP accumulates were imaged at ×63 on an Axioplan2 Epifluorescence Microscope (Zeiss) and thresholded in Metamorph software (Molecular Devices, CA, USA). $n = 5$ for each genotype.

2.10. Immuno-histochemistry

Anaesthetized Flies were decapitated and the brains dissected in PBS. Brains were fixed for 20 min with 4% formaldehyde in PBS with 0.4% Triton-X100, 10 mM EGTA and 50 mM $MgCl_2$ added. Brains were washed five times and incubated for 1 h with 10% Newborn Calfserum in PBS-T (PBS with 0.4% Triton-X100). Primary antibodies (anti-RFP, mouse, 1:100, abcam; anti-Tau, 1:2000, DAKO; anti-chaoptin, 1:50, DSHB, Iowa) were incubated at 4 °C. Washing consisted of five repetitions of 3 rinses and 20 min incubation with PBS-T. Secondary antibodies coupled to Alexa 488 or 568 (1:500 in PBS-T) were incubated overnight at 4 °C. After the final wash brains were embedded in Vectashield/70% Glycerol (3:1). For every genotype five brains were recorded using a Zeiss 710 confocal microscope using. Controls were imaged first and experimental brains were imaged with the same settings. Images were assembled using Photoshop.

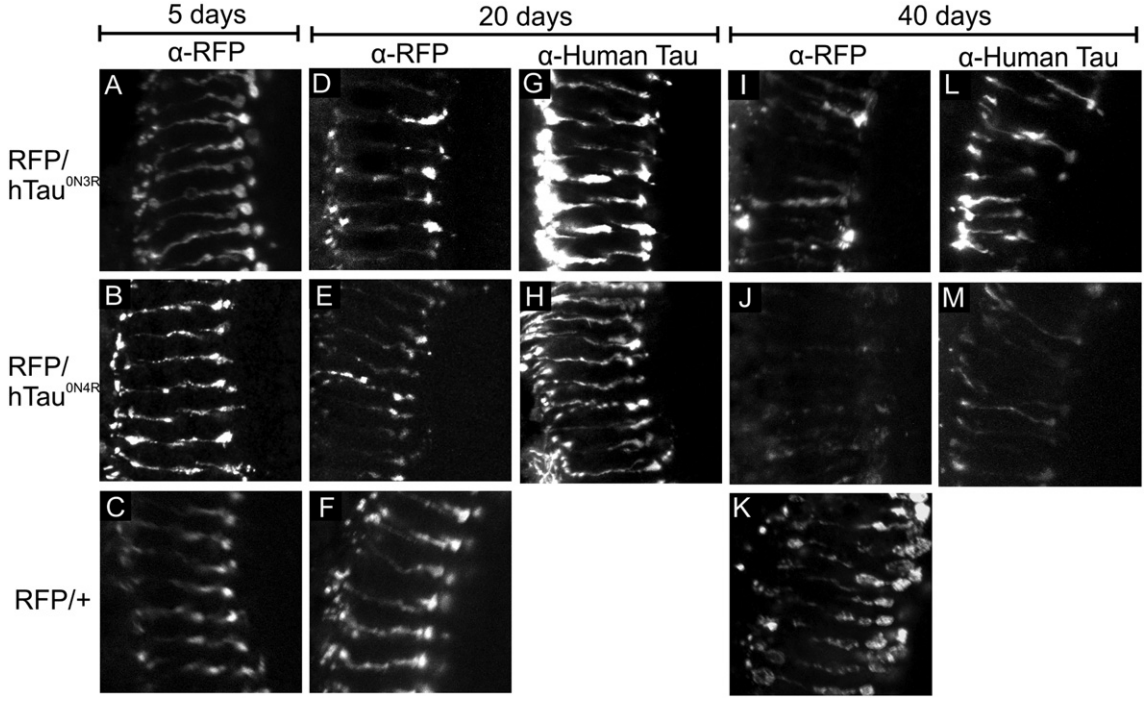

Fig. 3. The expression of 4 repeat human Tau disrupts R7 sensory neurons more severely than 3 repeat human Tau. R7 sensory neurons in the *Drosophila* visual system express the membrane marker myristolated-red fluorescent protein (myr-RFP) together with $hTau^{0N3R}$ (upper row), $hTau^{0N4R}$ (middle row) or on its own (RFP, bottom row). Adult brains were dissected 5 days (first column), 20 days (second and third column) or 40 days (fourth and fifth column) after eclosion. Brains were stained with antibodies against RFP or human tau (indicated at the top of each column). Images show axons in the medulla. Scale Bar = 10 μm. (A–C) In 5 day-old brains, RFP expression in R7 axons is not affected by the expression of either tau isoform. (D–F) In 20 day-old brains expression of $hTau^{0N3R}$ (D) and $hTau^{0N4R}$ (E) results in a weaker membrane RFP signal than in controls (F) but axons are still intact. (G, H) Expression of $hTau^{0N3R}$ (G) is stronger than $hTau^{0N4R}$ (H) and $hTau^{0N3R}$ shows a tendency to form aggregates at synapses. (I–K) In 40 day-old brains expressing either isoform (I, J) membrane RFP is severely reduced (compare I, J with K). In particular, $hTau^{0N4R}$ expression results in loss of RFP expression in broad areas in the medulla. (L, M) $hTau^{0N3R}$ (L) aggregates along the axons and at synapses and is still expressed stronger than $hTau^{0N4R}$ (M). $hTau^{0N3R}$ = {w / +; panR7-GAL4 / +; $UAShtau^{0N3R}$ / +}. $hTau^{0N4R}$ = {w / +; panR7-GAL4; $UAShTau^{0N4R}$ / + − parental line $hTau^{0N4R}$}. WT = {w / +; panR7-GAL4; + / +} on an OreR background.

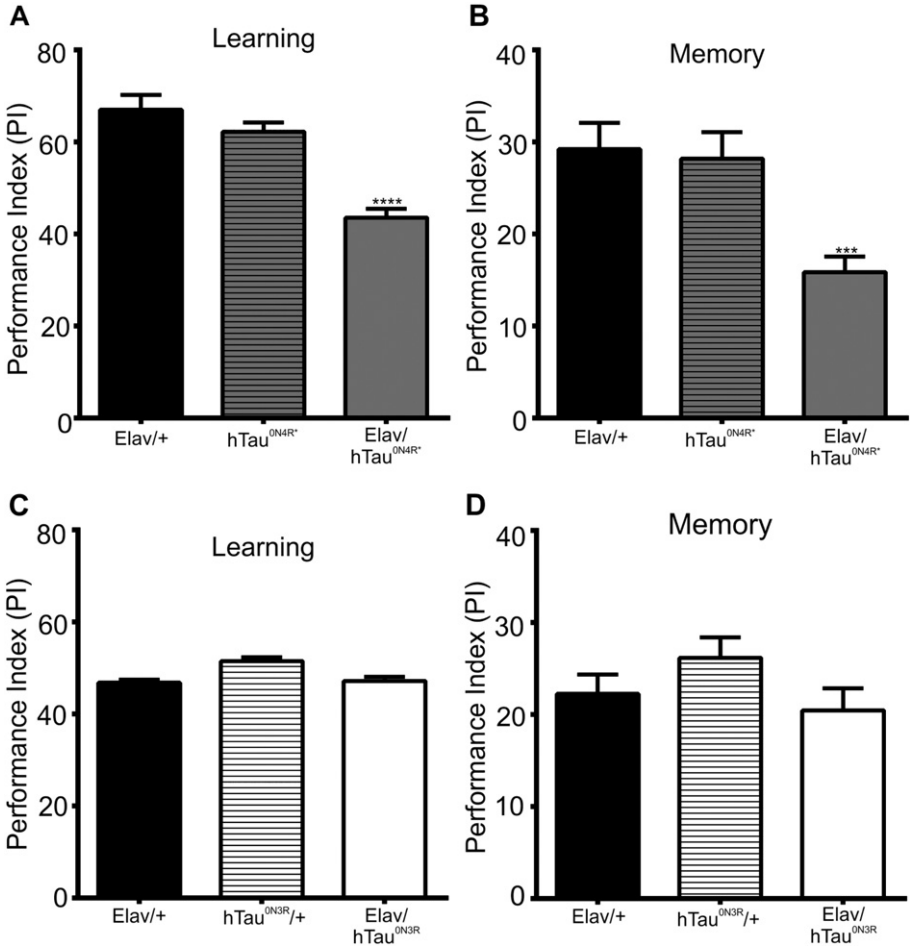

Fig. 4. The expression of 4 repeat human Tau impairs learning and memory but expression of 3R tau does not. Learning and associative memory was probed in transgenic lines in which adult specific expression of $hTau^{0N3R}$, $hTau^{0N4R}$ was driven by Elav-GAL4 / $TubGAL80^{ts}$. The transgenes were induced progeny of these crosses raised at 18 °C by transferring to 30 °C for 12 days prior to testing. Expression of $hTau^{0N4R}$ caused severe impairment in learning ($p < 0.001$, Dunnett's test, $n > 12$ per genotype) (A), and memory ($p < 0.001$, Dunnett's test, $n > 16$)(B), but expression of $hTau^{0N3R}$ did not affect either learning ($p = 0.4585$, Dunnett's test, $n > 12$)(C), or LTM ($p = 0.142$, Dunnett's test, $n > 14$ (D). $hTau^{0N3R}$ = {w / +; Elav-GAL4 / $TubGAL80^{ts}$ / +; $UAShtau^{0N3R}$ / +}. $hTau^{0N4R}$ = {w / +; GAL4 / $TubGAL80^{ts}$ / +; $UAShTau^{0N4R*}$ / + − parental line $hTau^{0N4R*}$}.

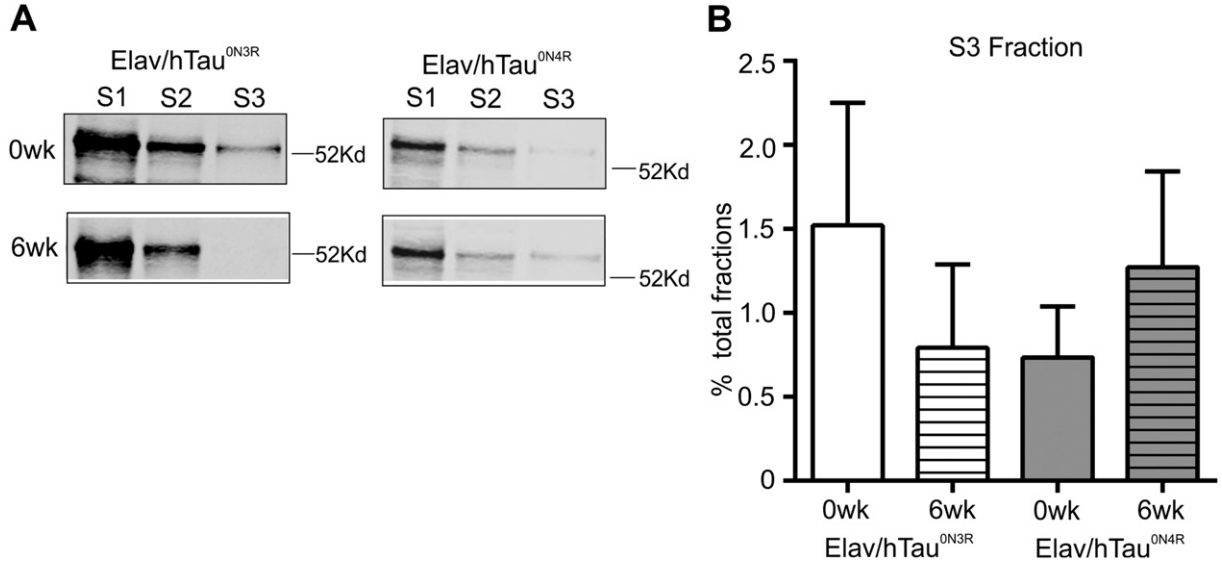

Fig. 5. No differences between 3R and 4R transgenics in the amount of insoluble tau oligomers formed with age. (A) Representative Western blots of soluble (S1), SDS-soluble (S2) and SDS-insoluble (S3) fractions generated from adult heads following Elav-GAL4 driven $hTau^{0N3R}$ and $hTau^{0N4R}$ expression in newly eclosed young (0 weeks) and old (6 weeks) flies. Some insoluble tau oligomeric species are detected in both young and old flies. B) However quantification of S3 fraction relative to sum total of all fractions shows there is no significant difference in the amount of insoluble tau between $hTau^{0N3R}$ and $hTau^{0N4R}$ expressing flies or with age in either line ($n = 4$). Unpaired, two-tailed *t*-tests used to test for significance. Error bars are plotted ±S.E.M. $hTau^{0N3R}$ = {w / +; Elav-GAL4 / +; $UAShTau^{0N3R}$ / +}. $hTau^{0N4R}$ = {w / +; Elav-GAL4 / +; $UAShTau^{0N4R}$ / + − parental line $hTau^{0N4R}$}. WT = {w / +; Elav-GAL4 / +; + / +} on an OreR background.

3. Results

3.1. Human 3-repeat tau and human 4-repeat tau expression present different phenotypes

To test whether the 0N3R and 0N4R isoforms yield identical, similar or distinct effects on larval mobility (Sinadinos et al., 2012), the UAS-hTau^{0N3R} and UAS hTau^{0N4R} transgenes were expressed in motor neurons under D42-GAL4. Using a semi-automated method to track larval locomotion (Sinadinos et al., 2012), we confirmed our previous observations that expression of hTau^{0N3R} in larval motor neurons manifests in locomotor defects. Significant impairments were evident in two larval locomotor parameters: meander and contractions (Fig. 1A–C), which arise from impaired axonal transport (Fig. 1D). In contrast, expression of hTau^{0N4R} did not result in significant locomotor deficits, or cause axonal transport impairments as profound as those induced by hTau^{0N3R} (Fig. 1A–D).

Isoform-specific phenotypes were also revealed in adult animals upon transgene expression with Elav-GAL4. Premature lethality was apparent in hTau^{0N3R}-expressing adult flies earlier than hTau^{0N4R}-expressing animals (Fig. 2A). In addition, isoform-specific differential effects were revealed on a negative geotaxis locomotor assay (Mudher et al., 2004) in adult flies expressing pan-neuronally the two tau isoforms. The climbing ability of flies expressing hTau^{0N3R} starts to decline at 1 week and diminishes rapidly as animals progress to week 5 and 6, when the majority of the flies are virtually immobile (Fig. 2B). By comparison, the climbing ability of flies expressing hTau^{0N4R} begins to deteriorate significantly one week later (week 2) and even at week 5, many of the flies remain mobile (Fig. 2B). Similar results were observed with an independent UAS-0N4R transgene insertion (Suppl. Fig. 2), supporting the idea that this difference between the tau isoforms is of biological significance and not because of differential expression levels due to transgene insertion. Therefore, expression of 0N3R tau appears to precipitate more severe effects than 0N4R expression in the same neurons.

Collectively the results indicate differential effects of the two tau isoforms on survival and larval and adult locomotion. Therefore, we wondered whether such differential isoform-specific effects may be revealed in additional neuronal subpopulations.

We selected a subset of eye sensory neurons to assay the effects of these isoforms since the fly retina has been used extensively to study tau-dependent neurodegeneration. Each tau isoform was co-expressed with membrane-tagged RFP (myristolated-RFP) in R7 sensory receptor neurons (pan-R7-GAL4). Degeneration was not apparent at 5 days post-eclosion evidenced by anti-RFP staining of axons following expression of either isoform (Fig. 3A–C). By day 20 however, degeneration was apparent in the sensory neurons expressing either of the isoforms, but with those expressing hTau^{0N4R} (Fig. 3E, H) presenting more extensive aberrations than those expressing hTau^{0N3R} (Fig. 3D, G). By 40 days post-eclosion, the sensory neurons expressing htau^{0N4R} had largely degenerated with only few axons remaining (Fig. 3J, M). In contrast, more axons remained in animals expressing hTau^{0N3R} at this time time-point (Fig. 3I, L). This data indicates that when expressed in the adult visual sensory neurons, hTau^{0N4R} exhibits a stronger neurodegenerative phenotype than hTau^{0N3R}. Interestingly, in 40 day-old hTau^{0N4R} brains myr-RFP expression is nearly absent (Fig. 3J), but accumulation of tau along the axons persists (Fig. 3M), indicating loss of membrane integrity leaving 'ghost' axonal scaffolds behind. We confirmed the loss of membrane integrity by expressing the tau isoforms in all photoreceptors (under GMR-GAL4) and using antibodies against the membrane glycoprotein Chaoptin (Hirai-Fujita et al., 2008). In 40 day-old hTau^{0N4R} expressing optic lobes, Chaoptin is completely absent, whereas although severely reduced in hTau^{0N3R} expressing neurons, it is still detectable (Suppl. Fig. 3). Therefore, the results from both myr-RFP and Chaoptin membrane markers confirm that although tau expression disrupts membrane integrity, the severity is isoform-specific with hTau^{0N4R} precipitating a stronger neurodegenerative phenotype than hTau^{0N3R}.

To further explore whether such isoform-dependent differences persisted in other adult assays, we undertook conditional pan neuronal expression of both isoforms in the adult CNS because hTau^{0N4R} expression has been reported to yield learning deficits in this assay (Papanikolopoulou and Skoulakis, 2015). Hence we investigated whether adult specific expression of 0N3R might also precipitate such deficits in learning and 24 h memory (long term memory-LTM). Surprisingly, while 0N4R expression impaired associative learning (Fig. 4A) in agreement with prior results (Papanikolopoulou and Skoulakis, 2015; Kosmidis et al., 2010) and LTM was similarly significantly impaired (Fig. 4B), expression of hTau^{0N3R} did not affect either of these processes (Fig. 4C, D).

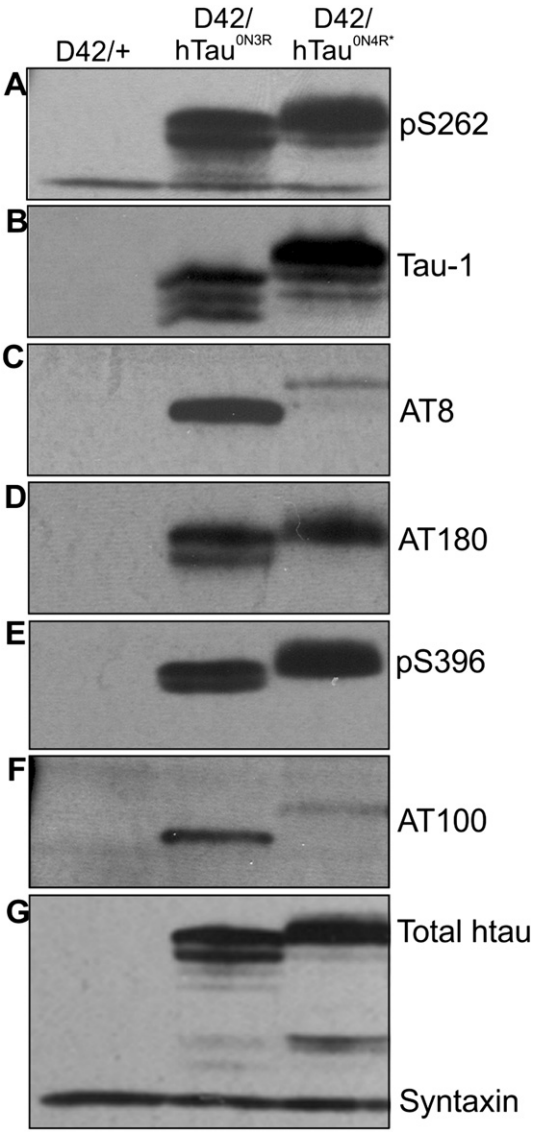

Fig. 6. Qualitative assessment of phosphorylation state in hTau^{0N3R} and hTau^{0N4R} larvae. Tau expression was driven using the D42-GAL4 motor neuron specific driver. Tau phosphorylation was assessed in wandering third instar larvae. Representative blots are shown for at least two independent experiments. Both isoforms of tau were phosphorylated to similar extents at the pS262 site (A), AT180 site (D) and pS396 site (E). However hTau^{0N4R*} was less phosphorylated at the AT8/Tau-1 site (B and C) and AT100 site (F). Expression of both isoforms of tau is comparable (G). hTau^{0N3R} = {w / +; D42-GAL4 / +; UAShTau^{0N3R} / +}. hTau^{0N4R} = {w / +; D42-GAL4 / +; UAShTau^{0N4R*} / + − parental line hTau^{0N4R*}}. WT = {w / +; D42-GAL4 / +; + / +} on an OreR background.

Collectively then, our data demonstrate that distinct larval and adult neuronal populations are differentially sensitive to the neuro-toxic effects of 0N3R and 0N4R tau isoforms, precipitating phenotypic strength differences, or lack of discernable phenotypes. This in turn strongly suggests that the effects of tau expression in *Drosophila* are not merely a consequence of non-specific toxicity or dysfunction due to overexpression of an exogenous protein. Rather it is likely that human tau isoforms interact differentially with the same or different intra-neuronal clients as suggested by the specificity and range of phenotypes described above.

3.2. Isoforms engage different mechanisms of toxicity

Differences in phenotypic strength can be precipitated by expression level differences. However this is unlikely to be key for the differences we report since the expression of the two tau isoforms is comparable in the transgenic lines we have employed (Suppl. Fig. 1). To investigate whether the two tau isoforms act differently at the cellular/molecular level, we assessed their accumulation, solubility, phosphorylation status and oxidative stress potential because these are other properties implicated in mechanisms of tau toxicity (Alavi Naini and Soussi-Yanicostas, 2015).

We have previously reported that increased tau levels lead to aggregation (Cowan et al., 2015) and accordingly we have found elevated accumulation of tau with increasing age in both 0N3R and 0N4R adults (data not shown). We therefore explored whether the age-dependent accumulation of tau led to its aggregation. Using a commonly used biochemical insolubility assay that enriches for insoluble oligomeric tau species (Cowan et al., 2015), we found little evidence of significant levels of insoluble tau oligomers in the brains of adult flies expressing 0N3R or 0N4R pan-neuronally, even in older flies (Fig. 5A). Though insoluble oligomeric tau species were not abundant, substantial isoform-specific aggregate profiles were not revealed upon fractionation of brain extracts expressing 0N3R or 0N4R (Fig. 5B). We did not investigate whether larger insoluble tau aggregates, such as tau filaments are found in these transgenics, because they have been described in some (Wu et al., 2013), but not all *Drosophila* tauopathy models (Wittmann et al., 2001).

Of the six isoforms, 0N3R is most highly phosphorylated (Smith et al., 1995), but whether the other tau isoforms undergo differential post-translational modifications has been unclear. Therefore we sought to determine whether the two isoforms were phosphorylated differentially in larval motor neurons implicated in the isoform-specific locomotor behaviours and in adult brains to potentially mirror the isoform-specific learning, memory and longevity differences. Hence, we expressed 0N3R or 0N4R specifically in larval motor neurons or adult brains and then probed the occupation status of a set of phosphorylation sites implicated in tauopathies.

Though phosphorylation at many sites was similar in larval motor neurons, there were some interesting isoform-specific differences. Phosphorylation at Ser 262 (Fig. 6A), Thr 231 (AT180 - Fig. 6D), and Ser 396 (Fig. 6E) did not appear significantly different between isoforms in larvae. However, the signal with the AT100 antibody appeared elevated in hTau^{0N3R}-expressing larvae (Fig. 6F). Phosphorylation at the AT8 site was also elevated in hTau^{0N3R}-expressing larvae, while in hTau^{0N4R}-expressing animals AT8 phosphorylation was suppressed as revealed by the Tau-1 antibody which is reactive to non-phosphorylated epitopes at the AT8 site (Fig. 6 B and C).

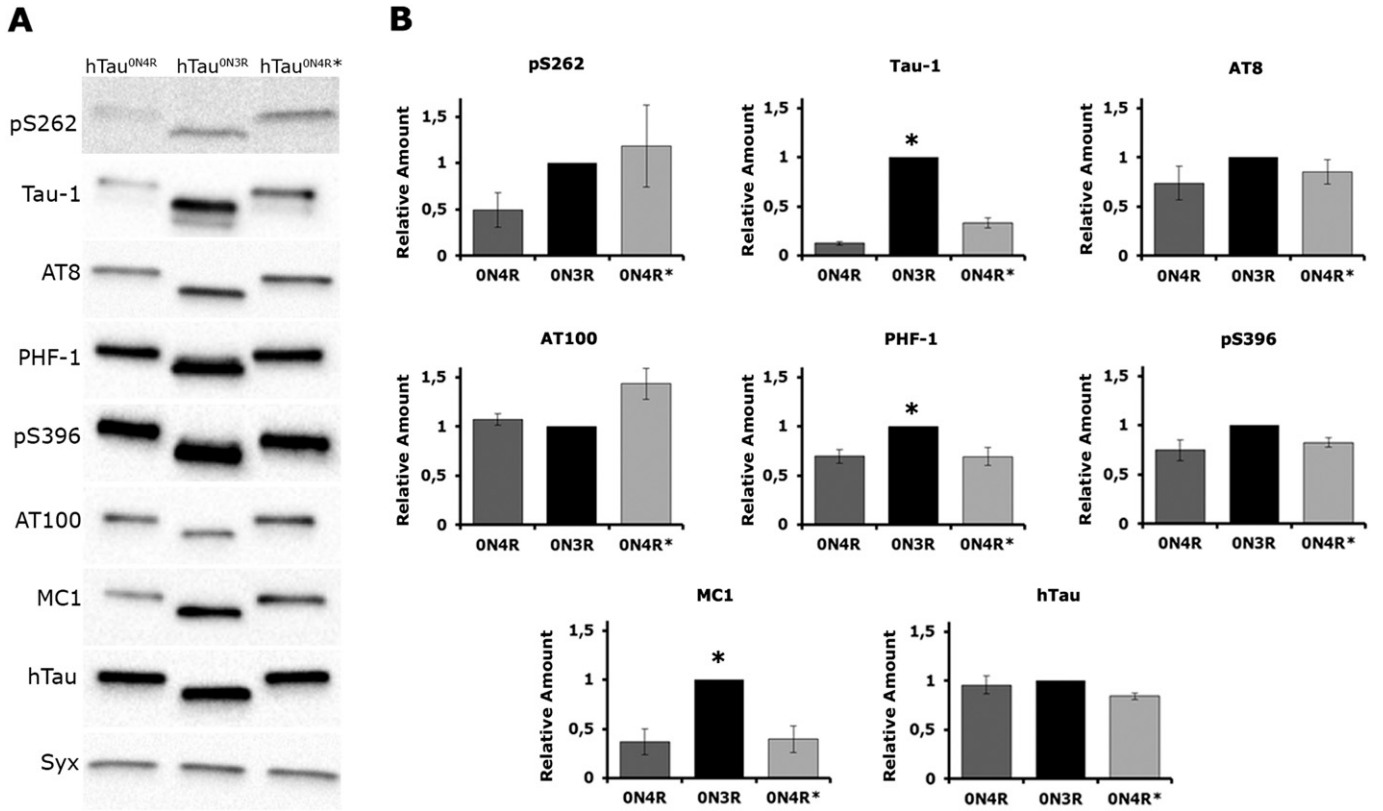

Fig. 7. Quantitative assessment of the phosphorylation state of hTau^{0N3R} and hTau^{0N4R} in adult brains. Tau expression was driven using the ELAV-GAL4 pan-neuronal driver. Tau phosphorylation was assessed in 1–3 day adult brains to compare 0N3R tau with two independent p-element insertion lines expressing 0N4R tau (referred to as hTau^{0N4R} and hTau^{0N4R*}). Representative blots are shown for at least three independent experiments (A) and their quantification is shown in (B). Both isoforms of tau were phosphorylated to similar extents at most sites except for the Tau-1 and PHF-1 sites which showed greater immunoreactivity in 0N3R tau brains. MC1 immunoreactivity, indicative of misfolded tau, was greater in 0N3R tau. Expression of total tau levels was comparable between all three lines. hTau^{0N3R} = {w / +; ELAV-GAL4 / +; UAShtau0N3R / +}. hTau^{0N4R} = {w / +; ELAV-GAL4 / +; UAShTau^{0N4R} / + − parental line hTau^{0N4R}} and hTau^{0N4R*} = {w / +; ELAV-GAL4 / +; UAShTau^{0N4R*} / + − parental line hTau^{0N4R*}}. WT = {w / +; ELAV-GAL4 / +; + / +} on an OreR background.

As with the larval motor neurons, the 0N3R and 0N4R isoforms were similarly phosphorylated at most epitopes in adult brain, but there were some interesting differences suggesting that developmental stage influences tau phosphorylation in an isoform-specific manner. These differences were genuine because they were evident even when the independent 0N4R p-element insertion line hTau^{0N4R*} was used (Fig. 7). In larval motor neurons, 0N3R tau is more phosphorylated than 0N4R tau at the AT8 site (as evidenced by increased AT8 and decreased Tau-1 immunoreactivity in 0N3R motor neurons) whereas in adult brain, 0N4R tau is more phosphorylated than 0N3R tau at these sites (as indicated by greater Tau-1 immunoreactivity in 0N3R brains) (Figs. 6 and 7). Similarly the greater phosphorylation of 0N3R tau at the AT100 site in larval motor neurons is not evident in adult brain (Figs 6 and 7). Instead, 0N3R tau is more phosphorylated at the Ser 396/404 (detected by PHF-1 with an increased trend seen with an antibody that only picks up phosphorylation at Ser 396) than 0N4R tau in adult brains but not in larval motor neurons (Figs 6 and 7). Significantly, the 0N3R isoform is much more immunoreactive with the MC1 antibody than the 0N4R proteins, suggesting differences in folding or pathology-related structure between the two isoforms.

In summary the data implies that 0N3R and 0N4R isoforms are differentially phosphorylated at some but not all sites in different developmental stages. Whether these site-specific phosphorylation differences underpin the differential phenotypes precipitated by the two isoforms is yet to be determined, but is consistent with the data. Moreover, because the phosphorylation profiles of these tau isoforms on tauopathy associated sites are not identical, the data support the notion of isoform-specific interactions with kinases and phosphatases.

Aside from phosphorylation and aggregation, oxidative stress is another mechanism by which tau mediates toxicity (Dias-Santagata et al., 2007; Alavi Naini and Soussi-Yanicostas, 2015). We therefore examined oxidative stress using a commercial assay to detect oxidised proteins in brain homogenates from flies expressing either tau isoform pan-neuronally. Though there was clear evidence of oxidative stress in brains from both transgenic lines, surprisingly, oxidation detected in hTau^{0N4R}-expressing flies was twice as much as of that detected in hTau^{0N3R}-expressing animals (Fig. 8). This again demonstrates a clear isoform-specific difference, which may underpin some of the isoform-specific differences in toxicity and neuronal dysfunction described here by us and by others in various tauopathy models.

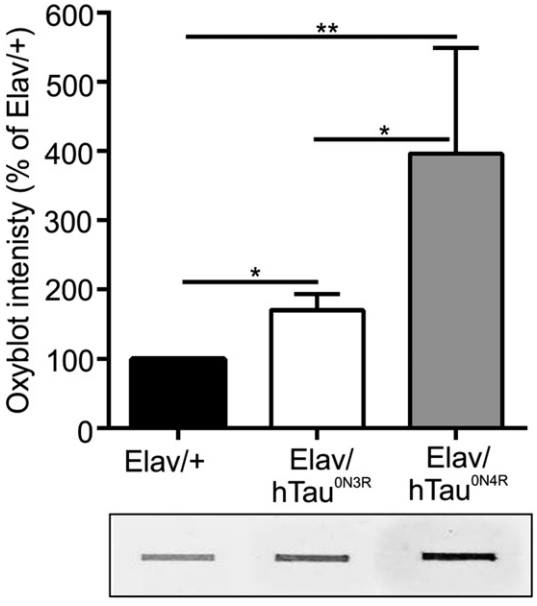

Fig. 8. Comparison of the protein oxidation induced by expression of hTau^{0N4R} versus hTau^{0N3R}-expressing *Drosophila*. Elav-GAL4 driven pan-neural expression of either hTau^{0N4R} or hTau^{0N3R} induces oxidative stress in 1d old adult flies as measured by a commercial Oxyblot assay. However levels of protein oxidation are significantly greater in hTau^{0N4R} versus hTau^{0N3R} flies. Graph represents the average of 9 experiments. Results from unpaired *t*-tests: wild-type vs hTau^{0N3R} $p = 0.0145$; hTau^{0N3R} vs hTau^{0N4R} $p = 0.04$; wild-type vs hTau^{0N4R} ($p = 0.008$). hTau^{0N3R} = {w / +; Elav-GAL4 / +; UAShTau^{0N3R} / +}. hTau^{0N4R} = {w / +; Elav-GAL4 / +; UAShTau^{0N4R} / + − parental line hTau^{0N4R}}. WT = {w / +; Elav-GAL4 / +; + / +} on an OreR background.

4. Discussion

We report here isoform-specific phenotypes in both larval and adult *Drosophila* expressing either hTau^{0N3R} or hTau^{0N4R} transgenes. Although expression level differences may contribute to the phenotypic consequences, isoform-specific differences independent of this were uncovered in this study. These results are in agreement with independent studies, which have also demonstrated isoform-specific differences in physiological tau biology, including sub-cellular localisation and function, and disease-relevant biochemical properties (Liu and Gotz, 2013; Liu et al., 2016).

Differences in the best-described cellular function of tau, microtubule binding, have long been known, and believed to arise because the 4R isoforms possess an extra microtubule-binding domain enabling three-fold greater microtubule affinity (Goode et al., 2000). However, the flanking carboxy-terminal region also differentially regulates microtubule-binding, and curiously appears to influence binding of 3R isoforms to a greater extent than 4R isoforms (Goode et al., 2000). In addition to microtubule-binding, isoform specific differences have been identified in several other physiological roles attributed to tau. This includes interacting partners, with 2N4R isoforms exhibiting stronger affinity to proteins implicated in neurodegeneration (Liu et al., 2016) and interactions with kinases such as Fyn, which binds preferentially to 3R tau (Bhaskar et al., 2005). Differences in sub-cellular localisation have also been uncovered, wherein 0N isoforms appear preferentially in the soma and axons, 1N isoforms in the dendrites and nucleus and 2N isoforms in cell bodies and axons (Liu and Gotz, 2013). Such results challenge the widely-held view that tau behaves preferentially as an axonal protein engaged mostly in microtubule stabilisation, and jointly with the data herein, promote the idea that tau is a protein of multiple functions which are likely sub-served differentially by distinct isoforms.

Further support for this notion is provided by isoform-specific differences in pathological behaviour including propensity to aggregate (Adams et al., 2010), morphology of aggregates formed (Adams et al., 2010) and templated seeding (Dinkel et al., 2011). Templated seeding of filaments in particular, exhibits striking isoform-specific barriers. While seeds containing 3R isoforms alone or 3R and 4R isoforms together can recruit both 3R and 4R monomers into growing filaments, seeds comprising just of 4R isoforms can only recruit 4R monomers (Dinkel et al., 2011). Since hyper-phosphorylation of tau is believed to promote its aggregation, some studies have explored the impact of pseudo-phosphorylation on aggregation in vitro and identified interesting isoform-specific differences (Combs et al., 2011). Although we have revealed isoform-specific, developmental stage-dependent phosphorylation differences, these do not appear to lead to aggregation differences, at least within the resolution afforded by our techniques, but clearly appear consistent with the distinct phenotypic consequences we detailed. Differences have also been reported in the sub-cellular localisation of the different tau isoforms and how this changes during the evolution of tangle pathology (Hara et al., 2013). Collectively these studies begin to elucidate why different tau isoforms are preferentially affected in different tauopathies and the cellular/molecular basis for predilection of different brain regions therein.

The studies discussed above show clear isoform-specific differences in the biochemical and pathological properties of tau; however not many studies have directly compared and contrasted isoform-specific

phenotypic differences in the same model. Adding to this, we show here that for some tau-mediated phenotypes, like axonal transport disruption and adult locomotion, the 3R tau isoform is more detrimental whereas in other tau-mediated phenotypes, such as learning and memory and photo-receptor degeneration, it is the 4R tau which is more toxic. In line with this, we have previously shown that expression of either hTau^{0N4R} or hTau^{2N4R} but not hTau^{0N3R} eliminates *Drosophila* mushroom bodies (Papanikolopoulou and Skoulakis, 2015; Grammenoudi et al., 2008; Papanikolopoulou et al., 2010), and that expression of hTau^{0N3R} is associated with dysfunction in the absence of neuronal death (Mudher et al., 2004; Cowan et al., 2010). Likewise, many other *Drosophila* models of tauopathy report degeneration, mainly of photoreceptors or other brain regions, but most studies invariably express 4R isoforms (Dourlen et al., 2016; Chanu and Sarkar, 2016). Moreover, to our knowledge, no other studies have directly compared the oxidative potential of 3R and 4R isoforms. We provide evidence that the 0N4R isoform is more potent at inducing oxidative stress than 0N3R. Oxidative stress has been reported in tauopathies implicating either or both 3R and 4R isoforms (reviewed in (Alavi Naini and Soussi-Yanicostas, 2015)). Whether, as our data suggests, it plays a more profound role in diseases involving 4R remains to be determined. In fact, of the few studies that have systematically compared 3R and 4R mediated phenotypes in the same model, work in mice suggests that tipping the balance towards 4R isoforms was associated with greater pathology and behavioural defects (Schoch et al., 2016).

The molecular mechanism(s) underpinning the divergent phenotypes of tau isoforms are unclear at present. Expression level and stability differences are likely contributing factors because tau-toxicity is generally believed to correlate with intraneuronal tau load (Ubhi et al., 2007). This notion is significantly supplemented and enhanced by our own results uncovering phenotypic differences between hTau^{0N3R} and hTau^{0N4R}, which persisted even in the face of comparable expression levels. Differences in the epitopes phosphorylated may be another contributing factor since such differences have been associated with differential toxicity (Brelstaff et al., 2015), or reduced microtubule binding (Biernat et al., 1993) which underpins tau-mediated neuronal dysfunction (Cowan et al., 2010; Quraishe et al., 2013).

5. Conclusion

The six tau isoforms are often regarded as the same protein. Indeed many of their normal biological and pathological characteristics are very similar. However, there are distinct differences in isoform functional properties arising from the variable N-terminal domains and 3 or 4 microtubule-binding domains. This manifests in variations in their post-translational regulation and in turn their normal cellular functions. Adding to this, we report here that they are distinctly different in their pathological potential as well. Such isoform-specific differences need to be taken into account when interpreting data from experimental models of tauopathy since they will invariably differ from model to model. It should also inform tau-centric therapeutic approaches. It remains to be investigated how the tau isoforms contribute to differential susceptibility of brain region and mechanism of tau-toxicity in different tauopathies.

Supplementary data to this article can be found online at http://dx.doi.org/10.1016/j.nbd.2017.05.003.

Acknowledgements

We would like to thank and acknowledge the Wessex Medical Trust and Gerald Kerkut Trust. This research has also been co-financed by the European Union (European Social Fund – ESF) and Greek national funds through the Operational Program "Education and Lifelong Learning" of the National Strategic Reference Framework (NSRF) - Research Funding Program: THALIS –UOA - "Study mechanisms of neurodegeneration in Alzheimer's disease".

References

Adams, S.J., DeTure, M.A., McBride, M., Dickson, D.W., Petrucelli, L., 2010. Three repeat isoforms of tau inhibit assembly of four repeat tau filaments. PLoS One 5, e10810. http://dx.doi.org/10.1371/journal.pone.0010810.

Alavi Naini, S.M., Soussi-Yanicostas, N., 2015. Tau hyperphosphorylation and oxidative stress, a critical vicious circle in neurodegenerative tauopathies? Oxidative Med. Cell. Longev.:151979 http://dx.doi.org/10.1155/2015/151979.

Andreadis, A., 2005. Tau gene alternative splicing: expression patterns, regulation and modulation of function in normal brain and neurodegenerative diseases. Biochim. Biophys. Acta 1739:91–103. http://dx.doi.org/10.1016/j.bbadis.2004.08.010.

Bhaskar, K., Yen, S.H., Lee, G., 2005. Disease-related modifications in tau affect the interaction between fyn and tau. J. Biol. Chem. 280:35119–35125. http://dx.doi.org/10.1074/jbc.M505895200.

Biernat, J., Gustke, N., Drewes, G., Mandelkow, E.M., Mandelkow, E., 1993. Phosphorylation of Ser262 strongly reduces binding of tau to microtubules: distinction between PHF-like immunoreactivity and microtubule binding. Neuron 11, 153–163.

Brelstaff, J., et al., 2015. The fluorescent pentameric oligothiophene pFTAA identifies filamentous tau in live neurons cultured from adult P301S tau mice. Front. Neurosci. 9:184. http://dx.doi.org/10.3389/fnins.2015.00184.

Chanu, S.I., Sarkar, S., 2016. Targeted downregulation of dMyc suppresses pathogenesis of human neuronal tauopathies in *Drosophila* by limiting heterochromatin relaxation and tau hyperphosphorylation. Mol. Neurobiol. http://dx.doi.org/10.1007/s12035-016-9858-6.

Combs, B., Voss, K., Gamblin, T.C., 2011. Pseudohyperphosphorylation has differential effects on polymerization and function of tau isoforms. Biochemistry 50:9446–9456. http://dx.doi.org/10.1021/bi2010569.

Cowan, C.M., Bossing, T., Page, A., Shepherd, D., Mudher, A., 2010. Soluble hyper-phosphorylated tau causes microtubule breakdown and functionally compromises normal tau in vivo. Acta Neuropathol. 120:593–604. http://dx.doi.org/10.1007/s00401-010-0716-8.

Cowan, C.M., et al., 2015. Rescue from tau-induced neuronal dysfunction produces insoluble tau oligomers. Sci. Report. 5:17191. http://dx.doi.org/10.1038/srep17191.

Dias-Santagata, D., Fulga, T.A., Duttaroy, A., Feany, M.B., 2007. Oxidative stress mediates tau-induced neurodegeneration in *Drosophila*. J. Clin. Invest. 117:236–245. http://dx.doi.org/10.1172/JCI28769.

Dinkel, P.D., Siddiqua, A., Huynh, H., Shah, M., Margittai, M., 2011. Variations in filament conformation dictate seeding barrier between three- and four-repeat tau. Biochemistry 50:4330–4336. http://dx.doi.org/10.1021/bi2004685.

Dourlen, P., et al., 2016. Functional screening of Alzheimer risk loci identifies PTK2B as an in vivo modulator and early marker of tau pathology. Mol. Psychiatry http://dx.doi.org/10.1038/mp.2016.59.

Goedert, M., Spillantini, M.G., Jakes, R., Rutherford, D., Crowther, R.A., 1989. Multiple isoforms of human microtubule-associated protein tau: sequences and localization in neurofibrillary tangles of Alzheimer's disease. Neuron 3, 519–526.

Goode, B.L., Chau, M., Denis, P.E., Feinstein, S.C., 2000. Structural and functional differences between 3-repeat and 4-repeat tau isoforms. Implications for normal tau function and the onset of neurodegenetative disease. J. Biol. Chem. 275:38182–38189. http://dx.doi.org/10.1074/jbc.M007489200.

Grammenoudi, S., Anezaki, M., Kosmidis, S., Skoulakis, E.M., 2008. Modelling cell and isoform type specificity of tauopathies in *Drosophila*. SEB Exp. Biol. Ser. 60, 39–56.

Hara, M., Hirokawa, K., Kamei, S., Uchihara, T., 2013. Isoform transition from four-repeat to three-repeat tau underlies dendrosomatic and regional progression of neurofibrillary pathology. Acta Neuropathol. 125:565–579. http://dx.doi.org/10.1007/s00401-013-1097-6.

Hirai-Fujita, Y., Yamamoto-Hino, M., Kanie, O., Goto, S., 2008. N-Glycosylation of the *Drosophila* neural protein Chaoptin is essential for its stability, cell surface transport and adhesive activity. FEBS Lett. 582:2572–2576. http://dx.doi.org/10.1016/j.febslet.2008.06.028.

Huefner, A., Kuan, W.L., Barker, R.A., Mahajan, S., 2013. Intracellular SERS nanoprobes for distinction of different neuronal cell types. Nano Lett. 13:2463–2470. http://dx.doi.org/10.1021/nl400448n.

Kosmidis, S., Grammenoudi, S., Papanikolopoulou, K., Skoulakis, E.M., 2010. Differential effects of tau on the integrity and function of neurons essential for learning in *Drosophila*. J. Neurosci. Off. J. Soc. Neurosci. 30:464–477. http://dx.doi.org/10.1523/JNEUROSCI.1490-09.2010.

Liu, C., Gotz, J., 2013. Profiling murine tau with 0N, 1N and 2N isoform-specific antibodies in brain and peripheral organs reveals distinct subcellular localization, with the 1N isoform being enriched in the nucleus. PLoS One 8, e84849. http://dx.doi.org/10.1371/journal.pone.0084849.

Liu, C., Song, X., Nisbet, R., Gotz, J., 2016. Co-immunoprecipitation with tau isoform-specific antibodies reveals distinct protein interactions and highlights a putative role for 2N tau in disease. J. Biol. Chem. 291:8173–8188. http://dx.doi.org/10.1074/jbc.M115.641902.

Medina, M., Hernandez, F., Avila, J., 2016. New features about tau function and dysfunction. Biomolecules 6. http://dx.doi.org/10.3390/biom6020021.

Mudher, A., et al., 2004. GSK-3beta inhibition reverses axonal transport defects and behavioural phenotypes in *Drosophila*. Mol. Psychiatry 9:522–530. http://dx.doi.org/10.1038/sj.mp.4001483.

Niblock, M., Gallo, J.M., 2012. Tau alternative splicing in familial and sporadic tauopathies. Biochem. Soc. Trans. 40:677–680. http://dx.doi.org/10.1042/BST20120091.

Papanikolopoulou, K., Skoulakis, E.M., 2015. Temporally distinct phosphorylations differentiate tau-dependent learning deficits and premature mortality in *Drosophila*. Hum. Mol. Genet. 24:2065–2077. http://dx.doi.org/10.1093/hmg/ddu726.

Papanikolopoulou, K., Kosmidis, S., Grammenoudi, S., Skoulakis, E.M., 2010. Phosphorylation differentiates tau-dependent neuronal toxicity and dysfunction. Biochem. Soc. Trans. 38:981–987. http://dx.doi.org/10.1042/BST0380981.

Park, S.A., Ahn, S.I., Gallo, J.M., 2016. Tau mis-splicing in the pathogenesis of neurodegenerative disorders. BMB Rep.

Quraishe, S., Cowan, C.M., Mudher, A., 2013. NAP (davunetide) rescues neuronal dysfunction in a *Drosophila* model of tauopathy. Mol. Psychiatry 18:834–842. http://dx.doi.org/10.1038/mp.2013.32.

Rabano, A., Cuadros, R., Calero, M., Hernandez, F., Avila, J., 2013. Specific profile of tau isoforms in argyrophylic grain disease. Exp. Neurosci. 7:51–59. http://dx.doi.org/10.4137/JEN.S12202.

Schoch, K.M., et al., 2016. Increased 4R-tau induces pathological changes in a human-tau mouse model. Neuron 90:941–947. http://dx.doi.org/10.1016/j.neuron.2016.04.042.

Sinadinos, C., Cowan, C.M., Wyttenbach, A., Mudher, A., 2012. Increased throughput assays of locomotor dysfunction in *Drosophila* larvae. J. Neurosci. Methods 203:325–334. http://dx.doi.org/10.1016/j.jneumeth.2011.08.037.

Smith, C.J., Anderton, B.H., Davis, D.R., Gallo, J.M., 1995. Tau isoform expression and phosphorylation state during differentiation of cultured neuronal cells. FEBS Lett. 375, 243–248.

Spillantini, M.G., Goedert, M., 2013. Tau pathology and neurodegeneration. Lancet Neurol. 12:609–622. http://dx.doi.org/10.1016/S1474-4422(13)70090-5.

Ubhi, K.K., Shaibah, H., Newman, T.A., Shepherd, D., Mudher, A., 2007. A comparison of the neuronal dysfunction caused by *Drosophila* tau and human tau in a *Drosophila* model of tauopathies. Invertebr. Neurosci. 7:165–171. http://dx.doi.org/10.1007/s10158-007-0052-4.

Wittmann, C.W., et al., 2001. Tauopathy in *Drosophila*: neurodegeneration without neurofibrillary tangles. Science 293:711–714. http://dx.doi.org/10.1126/science.1062382.

Wu, T.H., et al., 2013. Loss of vesicular dopamine release precedes tauopathy in degenerative dopaminergic neurons in a *Drosophila* model expressing human tau. Acta Neuropathol. 125:711–725. http://dx.doi.org/10.1007/s00401-013-1105-x.